

# SYNTHESIS AND *IN SILICO* APPROACHES OF NEW SYMMETRIC BIS-THIAZOLIDINE-2,4-DIONES AS Ras AND Raf ONCOPROTEINS INHIBITORS

OVIDIU CRIȘAN<sup>1</sup>, GABRIEL MARC<sup>2\*</sup>, CRISTINA NASTASĂ<sup>2</sup>, SMARANDA ONIGA<sup>3</sup>, LAURIAN VLASE<sup>4</sup>, ADRIAN PÎRNĂU<sup>5</sup>, OVIDIU ONIGA<sup>2</sup>

<sup>1</sup>Department of Organic chemistry, Faculty of Pharmacy, "Iuliu Hațieganu" University of Medicine and Pharmacy, 41 Victor Babeș Street, 400012, Cluj-Napoca, Romania

<sup>2</sup>Department of Pharmaceutical chemistry, Faculty of Pharmacy, "Iuliu Hațieganu" University of Medicine and Pharmacy, 41 Victor Babeș Street, 400012, Cluj-Napoca, Romania

<sup>3</sup>Department of Therapeutical chemistry, Faculty of Pharmacy, "Iuliu Hațieganu" University of Medicine and Pharmacy, 12 Ion Creangă Street, 400010, Cluj-Napoca, Romania

<sup>4</sup>Department of Biopharmacy, Faculty of Pharmacy, "Iuliu Hațieganu" University of Medicine and Pharmacy, 41 Victor Babeș Street, 400012, Cluj-Napoca, Romania

<sup>5</sup>National Institute for Research and Development of Isotopic and Molecular Technologies, 67-103 Donat Street, 400293 Cluj-Napoca, Romania

\*corresponding author: marc.gabriel@umfcluj.ro

Manuscript received: November 2022

## Abstract

Millions of people die of cancer every year, all around the world. Unfortunately, the conventional chemotherapy is associated with some pharmacotoxicological inconveniences. Due to this fact, the discovery of new anticancer agents is needed, with better activity and selectivity of action at the level of the tumour microenvironment. Thiazolidinediones, known mainly as antihyperglycemic substances, are more and more investigated for their antiproliferative properties. Prompted by our interest and experience in synthesizing new small molecules with biological potential, we present here the chemical synthesis of a new series of symmetric bis-5-arylidene-thiazolidine-2,4-diones. The molecular docking performed on K-Ras, N-Ras and B-Raf oncoproteins revealed a promising binding affinity to K-Ras, especially for the compounds **5b** and **5h**. A molecular dynamics simulation was made for the complexes of the two compounds with K-Ras oncoprotein, to predict the stability of the resulted complexes.

## Rezumat

Milioane de oameni mor anual din cauza cancerului, în întreaga lume. Din păcate, chimioterapia convențională este asociată cu unele inconveniente de ordin farmacotoxicologic. Din cauza acestui neajuns, este necesară descoperirea de noi agenți anticanceroși, cu activitate superioară și selectivitate de acțiune la nivelul micromediului tumoral. Tiazolidindionele, cunoscute în principal ca substanțe antihiperliceminate, sunt din ce în ce mai mult cercetate pentru proprietățile lor antiproliferative. Ca urmare a interesului și a experienței noastre în sinteza unor noi molecule mici cu potențial biologic, prezentăm aici sinteza chimică a unei noi serii de bis-5-aryliden-tiazolidin-2,4-dione. Andocarea moleculară realizată pe oncoproteinele K-Ras, N-Ras și B-Raf a arătat o afinitate de legare de K-Ras promițătoare, în special pentru compușii **5b** și **5h**. O simulare de dinamică moleculară a fost realizată pentru aceste două substanțe, pentru a prezice stabilitatea complexelor formați cu oncoproteina K-Ras.

**Keywords:** thiazolidine-2,4-diones, Ras, Raf inhibitors, anticancer agents

## Introduction

The incidence of malignancies has risen in the last years, in a very dramatic way. Nowadays, cancer ranks as top reason for death, all over the world [6]. The current chemotherapy comes with some notable disadvantages, such as the failure in prolonging life expectancy, toxic effects, lack of selectivity and drug-resistance, due to the long period of therapy in some cases [53]. Therefore, the improvement of the existent antitumor treatment, the discovery of new active agents, with less toxicity and higher selectivity of action and

the identification of new molecular targets are urgently needed. Despite the efforts made in searching new therapeutic strategies and cellular signalization pathways, malignant cells are constantly developing resistance to these anticancer agents. Therefore, alternative therapies should be targeted, in order to overcome the drug-resistance problem.

Currently, there is a great interest in the development of new small molecules such as thiazolidinediones (TZDs), for the treatment of various types of cancer. Recent literature data indicate that some TZD members

exhibit promising antiproliferative activities and limit the progress of metastasis, both *in vitro* and *in vivo* studies, in lung, breast and pancreatic cancers [11, 14, 43]. Rosiglitazone, ciglitazone and pioglitazone, which contain the thiazolidine-2,4-dione scaffold, have demonstrated an antitumor effect in preclinical studies and a beneficial role in several clinical trials [7, 16, 26, 45, 47]. The outcomes of these trials with glitazones used alone or in association with a well-known anticancer drug, have been very promising, encouraging more studies of TZDs in tumour diseases [34, 44]. Furthermore, the newer analogues, such as efatutazone or lobeglitazone, have been investigated for their efficiency in thyroid cancer [20, 47].

Thiazolidine-2,4-diones act mainly as agonists of Peroxisome Proliferator-Activated Receptor- $\gamma$  (PPAR- $\gamma$ ) and their main therapeutic use is in the oral treatment of diabetes 2. Many studies done in the last years focused on understanding the anticancer mechanism of action of these compounds. Although TZDs have been regarded as PPAR- $\gamma$  ligands, the antitumor effect demonstrated can be attributed only in part to genomic PPAR- $\gamma$  activation. Scientific data present various pathways and subsequent cancer hallmarks affected by TZDs in PPAR- $\gamma$  dependent and in independent way, resulting in downregulation of cancer cell proliferation, migration capacity, inflammatory responses, angiogenesis, invasive ability, and in up-regulation of apoptosis of cancerous cells [4, 8, 10, 12, 39, 54]. Thereby, thiazolidine-2,4-dione derivatives possess the capacity to reduce the growth of cancer cells at multiple check points involved in various action pathways, so, they can be considered important and better therapeutic alternatives to current single targeting drugs. The significance of PI3K/Akt and Ras-Raf-MEK1/MEK2-ERK1/ERK2 pathways in the aetiology of human cancers has led to the consideration of different members of these signalling pathways for drug discovery research [33]. Thiazolidinediones have also been reported as potential PI3K and MEK inhibitors, revealing a dual activity [1, 25].

From the chemical point of view, thiazolidine-2,4-dione is a five-membered heterocycle, containing a cyclic amide function and an acidic -NH group. This scaffold is very fascinating for the medicinal chemists due to its numerous structural diversification opportunities which come along with a broad spectrum of biological activities, especially as anticancer agents [1, 5, 40]. The signature reaction of TZD is Knoevenagel condensation, in order to obtain 5-arylidene derivatives. The presence of the acidic group -NH allows an easy N-substitution, when reacted with alkyl/benzyl/acetyl halides, in basic medium [48, 51].

Molecular hybridization represents a modern approach in the rational design of multitargeting agents, by connecting two or more pharmacophore entities in one single molecule. This concept is based on the combination of pharmacophoric moieties from different

bioactive compounds, with the aim of producing a new hybrid molecule displaying enhanced efficacy, in comparison with the parent substances [9, 13, 52]. Furthermore, this drug development strategy can result in molecules with modified target selectivity profiles, different or multi modes of action, and the potential diminution of the undesired side effects of therapy. The study of TZD hybrids from the point of view of their *in silico* design, chemical synthesis, investigation of their antitumor, antidiabetic, anti-inflammatory, antioxidant and antimicrobial activities, has enabled the discovery of very promising and drug-like candidates.

Considering the aspects presented above and our previous experience in the synthesis of hybrid thiazolidine-2,4-dione derivatives and in the investigation of their antimicrobial [30, 36], anti-inflammatory [38], antioxidant [18, 31] and antitumour [37] potential, our aim in this work was to obtain new symmetric bis-thiazolidine-2,4-diones and to evaluate, *in silico*, their capacity to inhibit Raf and Ras oncoproteins, as potential antitumor drug candidates.

## Materials and Methods

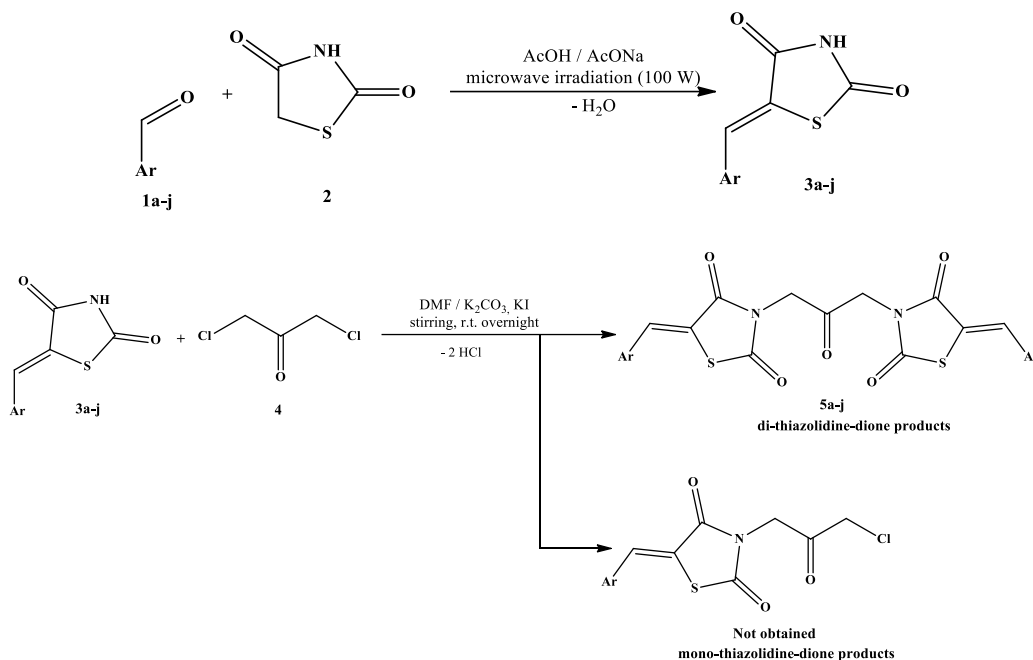
### Chemistry

Reagents and solvents used for synthesis had analytical grade purity and were purchased from local suppliers and were used without any supplementary processing. The microwave synthesis of the intermediate compounds **3a-j** was performed using a Discover BenchMate (CEM, Matthews, NC, USA) reactor under condenser at atmospheric pressure. The purity of the intermediate and final compounds was assessed using TLC and HPLC. The mass spectra of the intermediate and final compounds were recorded on an Agilent 1100 device, in positive ionization mode using an Agilent Ion Trap SL mass spectrometer (Agilent Technologies, Santa Clara, CA, USA). The melting points of the final compounds were determined using an MPM-H1 melting point device (Schorpp Gerätetechnik, Überlingen, Germany). The infrared spectra of the intermediate and final compounds were recorded using a FT/IR 6100 spectrometer (Jasco, Cremella, Italy) in KBr. The  $^1\text{H-NMR}$  and  $^{13}\text{C-NMR}$  spectra were recorded using an Avance NMR spectrometer (Bruker, Karlsruhe, Germany) in dimethyl sulfoxide- $d_6$ . Chemical shift values were reported in  $\delta$  units, using tetramethyl silane for calibration.

The route of synthesis followed to obtain the final compounds **5a-j** is presented in Figure 1. Firstly, the intermediate compounds **3a-j** were obtained after a Knoevenagel condensation between some (hetero)-aromatic aldehydes (**1a-j**) and thiazolidine-2,4-dione (**2**) using a previously reported protocol [30, 46, 55]. To obtain the final compounds **5a-j**, 2 mmol of intermediate compounds **3a-j** were mixed with 1 mmol (0.127 g) of 1,3-dichloroacetone (**4**), 1 mmol

(0.166 g) of anhydrous KI and 2 mmol (0.276 g) of  $K_2CO_3$  in 5 mL of DMF in a glass flask as previously reported by our group [32]. The reaction flask was closed and mixed well overnight. The progress of the reaction was monitored using TLC. After completion of the reaction, the reaction mixture was poured over

ice and diluted HCl was added dropwise until neutrality and total precipitation of the reaction product. The crude solid was filtered using a suction funnel and left to dry. The final compounds **5a-j** were obtained after crystallization of the corresponding crude solids from acetone.



**1a, 3a, 5a:** Ar =  $C_6H_5$

**1b, 3b, 5b:** Ar =  $C_6H_4-4-F$

**1c, 3c, 5c:** Ar =  $C_6H_4-4-NO_2$

**1d, 3d, 5d:** Ar =  $C_6H_4-2-OCH_3$

**1e, 3e, 5e:** Ar =  $C_6H_4-4-OCH_3$

**1f, 3f, 5f:** Ar =  $C_6H_4-4-Cl$

**1g, 3g, 5g:** Ar =  $C_6H_4-3-Cl$

**1h, 3h, 5h:** Ar =  $C_6H_3-2,4-diCl$

**1i, 3i, 5i:** Ar = 3-pyridyl

**1j, 3j, 5j:** Ar = 2-thiophenyl

**Figure 1.**

The synthetic route followed to obtain the final compounds **5a-j**

#### *In silico affinity evaluation*

The *in silico* evaluation of the affinity of the compounds **5a-j** to K-Ras, N-Ras and B-Raf was performed following a twostep protocol, in order to avoid the false positive results [24, 28]. The initial molecular docking study was performed using AutoDock vina 1.1.2 [49]. The same dataset of compounds was targeted against the same proteins using AutoDock 4.2 [35] for the validation of the AutoDock vina results. The top binding compounds were subjected to a molecular dynamics study to evaluate the stability of the predicted complexes produced by AutoDock vina. Preparation of the files of the ligands was performed according to the previously reported protocol using AutoDockTools 1.5.6. from MGLTools, Open Babel 2.4.1 and Avogadro 1.2.0 [15, 35, 41].

#### *Molecular docking*

In order to evaluate the affinity of the compounds **5a-j** to K-Ras, N-Ras and B-Raf, an *in silico* molecular

docking study was performed using AutoDock vina 1.1.2 (ADV) [49]. The three-dimensional structures of the targeted proteins were taken from RCSB Protein Data Bank (PDB) [3]. The molecular docking studies were performed against the A chain fragment of the deposited macromolecules, with the proper preliminary preparation of the macromolecules, according to the previously reported protocol [30, 35]. 20 poses were generated for each ligand in all three macromolecules binding sites. The macromolecules used in the study were deposited in the PDB with the codes 7EWB (K-Ras), 6ZIZ (N-Ras) and 5ITA (B-Raf) [22, 23, 29]. The search space for all proteins was defined as a cube, with the sides equal to 22. The choice of the parameters of the search space was made in order to fit the co-crystallized ligands found from the deposited complexes. The centre of the search space was defined by the cartesian coordinates as  $x = -2.197$ ,  $y = -11.099$ ,  $z = 11.469$  for 7EWB,  $x = 35.571$ ,  $y = -3.461$ ,  $z = 31.219$

for 6ZIZ and  $x = 27.622$ ,  $y = -1.952$ ,  $z = -19.823$  for 5ITA, respectively.

For AutoDock 4.2 (AD) the grid point spacing was set to 0.375 Å and the size of the search space was set to 54 points on each side of the cube. The centre coordinates of the search space were kept as presented for AutoDock vina 1.1.2. For each ligand AutoDock 4.2 searched for 200 poses in the binding sites of the targeted proteins.

The visualization of the results of the molecular docking study was performed using Chimera 1.10.2 [42].

#### Molecular dynamics simulation

The molecular dynamics simulations were performed with GROMACS 2022 [2] using CHARMM36 force field [17] and the TIP3P water model in a orthorhombic box [21]. GROMACS was installed on a machine running Debian 11, equipped with an Intel Core 7700K CPU for performing the computational tasks with *Compute Unified Device Architecture* (CUDA) for GPU acceleration using a NVIDIA RTX 3060.

The simulated systems were constructed, neutralized and relaxed by energy minimization according to the previous works reported and the simulations were run for 100 ns [19, 27].

## Results and Discussion

### Chemistry

The structures of the final compounds **5a-j** were confirmed by the spectral data recorded (MS, FT-IR,  $^1\text{H}$  NMR,  $^{13}\text{C}$  NMR), agreeing with the expected results. In the IR spectrum of the compounds, three peaks given by the  $\nu\text{C=O}$  were identified between 1742 - 1671  $\text{cm}^{-1}$ , as a general characteristic for all the studied compounds. Particularly, some specific signals were identified in the IR spectrum of some compounds: a strong signal at 1248  $\text{cm}^{-1}$  in compound **5b**, given by the  $\nu\text{C-F}$  bond; two strong signals at 1538  $\text{cm}^{-1}$  and 1347  $\text{cm}^{-1}$  given by the  $\nu\text{N-O}$  bond from the nitro group in compound **5c**, two strong signals at 1255  $\text{cm}^{-1}$  and 1028  $\text{cm}^{-1}$  given by the ether group in compound **5d** and other two strong signals at 1264  $\text{cm}^{-1}$  and 1027  $\text{cm}^{-1}$  given by the ether group in compound **5e**.

In the NMR spectra of the compounds **5a-j**, the signals in the expected regions were found, with the expected integrals and multiplicity. Analysis of the IR and  $^{13}\text{C}$  NMR spectra does not bring conclusive information to clarify the successful obtaining of the desired structures as di-thiazolidinedione or mono-thiazolidinedione products, while MS and  $^1\text{H}$  NMR spectra can be used to confirm the obtaining of the di-thiazolidinedione products. The ratio between the integrals of the peaks in the  $^1\text{H}$  NMR spectra, between the protons from the methylene groups from the propanone linker and the aromatic substituent of the thiazolidinedione, is the expected one. More than that, the four protons from the methylene groups

from the propanone linker appear as a unique singlet, while if the obtained compounds were mono-thiazolidinedione derivatives they would appear as two singlets, corresponding to two protons each.

The theoretical mono-thiazolidinedione derivatives depicted in Figure 1 were not obtained, not even in traces, the reaction giving the symmetric di-thiazolidinedione derivatives in high yields. Therefore, we can conclude that the obtaining of the corresponding  $\alpha$ -chloro ketone compounds (mono-thiazolidinediones) cannot be made under these reaction conditions and it would be necessary to use another synthetic route. Supplementary (data not provided), we tried to increase the amount of 1,3-dichloropropanone (**4**), reaching even a 1:10 ratio between the intermediate compound **3e** and 1,3-dichloropropanone (**4**) in the same experimental conditions, but still only the **5d** was isolated and no corresponding mono-thiazolidinedione was identified. As we observed before, the acidic nitrogen from the imide group of thiazolidinedione is easily substituted with an aliphatic halide reagent, *via* a  $\text{S}_{\text{N}}2$  mechanism, in alkaline environment [32].

Compound **5a** was previously reported in the literature, but it was obtained using another synthetic route.

(*Z*)-3,3'-(2-oxopropane-1,3-diyl)bis(5-((*Z*)-benzylidene)thiazolidine-2,4-dione) (**5a**): white solid; mp = 240 - 241 °C (lit. 240 °C [50]); yield = 88%; IR (KBr)  $\nu_{\text{max}}$   $\text{cm}^{-1}$ : 1735 (C=O), 1699 (C=O), 1685 (C=O), 1607 (C=C); MS: m/z = 465.1 (M+1);  $^1\text{H}$  NMR (DMSO- $d_6$ , 500 MHz)  $\delta$ : 4.99 (s, 4H,  $-\text{CH}_2-$ ), 7.19 (t, 2H, Ar,  $J = 7.5$  Hz), 7.60 - 7.62 (m, 4H, Ar), 7.89 (s, 2H,  $-\text{CH=}$ );  $^{13}\text{C}$  NMR (DMSO- $d_6$ , 125 MHz)  $\delta$ : 48.24 ( $-\text{CH}_2-$ ), 121.19 (TZD), 122.19 ( $-\text{CH=}$ ), 128.77 (Ar), 129.51 (Ar), 132.86 (Ar), 133.55 (Ar), 164.29 (TZD C=O), 167.02 (TZD C=O), 195.71 (C=O).

(*Z*)-3,3'-(2-oxopropane-1,3-diyl)bis(5-((*Z*)-4-fluorobenzylidene)thiazolidine-2,4-dione) (**5b**): white solid; mp = 260 - 261 °C; yield = 53%; IR (KBr)  $\nu_{\text{max}}$   $\text{cm}^{-1}$ : 1738 (C=O), 1696 (C=O), 1684 (C=O), 1597 (C=C), 1248 (C-F); MS: m/z = 501.2 (M+1);  $^1\text{H}$  NMR (DMSO- $d_6$ , 500 MHz)  $\delta$ : 4.98 (s, 4H,  $-\text{CH}_2-$ ), 7.49 (d, 4H, Ar,  $J = 7$  Hz), 7.68 (d, 4H, Ar,  $J = 7$  Hz), 8.00 (s, 2H,  $-\text{CH=}$ );  $^{13}\text{C}$  NMR (DMSO- $d_6$ , 125 MHz)  $\delta$ : 48.01 ( $-\text{CH}_2-$ ), 117.50 (Ar,  $J = 20$  Hz), 124.10 (TZD), 126.89 ( $-\text{CH=}$ ), 129.98 (Ar), 134.69 (Ar), 163.50 (Ar  $J = 250$  Hz), 164.91 (TZD C=O), 166.88 (TZD C=O), 195.29 (C=O).

(*Z*)-3,3'-(2-oxopropane-1,3-diyl)bis(5-((*Z*)-4-nitrobenzylidene)thiazolidine-2,4-dione) (**5c**): yellow solid; mp = 285 - 288 °C dec; yield = 89%; IR (KBr)  $\nu_{\text{max}}$   $\text{cm}^{-1}$ : 1739 (C=O), 1704 (C=O), 1686 (C=O), 1612 (C=C), 1538 (N=O), 1347 (N=O);  $^1\text{H}$  NMR (DMSO- $d_6$ , 500 MHz)  $\delta$ : 5.00 (s, 4H,  $-\text{CH}_2-$ ), 8.05 (s, 2H,  $-\text{CH=}$ ), 8.11 (d, 4H, Ar,  $J = 7.5$  Hz), 8.44 (d, 4H, Ar,  $J = 7.5$  Hz);  $^{13}\text{C}$  NMR (DMSO- $d_6$ , 125 MHz)  $\delta$ : 48.82 ( $-\text{CH}_2-$ ), 123.38 (Ar), 124.19 (TZD), 126.16

(-CH=), 130.19 (Ar), 144.05 (Ar), 149.31 (Ar), 164.83 (TZD C=O), 166.56 (TZD C=O), 195.44 (C=O).

(*Z*)-3,3'-(2-oxopropane-1,3-diyl)bis(5-((*Z*)-2-methoxybenzylidene)thiazolidine-2,4-dione) (**5d**): yellow solid; carbonization over 235°C; yield = 82%; IR (KBr)  $\nu_{\max}$  cm<sup>-1</sup>: 1739 (C=O), 1697 (C=O), 1685 (C=O), 1593 (C=C), 1255 (Ar-O-C), 1028 (Ar-O-C); MS: *m/z* = 542.2 (M+23); <sup>1</sup>H NMR (DMSO-*d*<sub>6</sub>, 500 MHz)  $\delta$ : 4.97 (s, 4H, -CH<sub>2</sub>-), 7.12 (t, 2H, Ar, *J* = 7.5 Hz), 7.18 (d, 2H, Ar, *J* = 8.5 Hz), 7.47 (dd, 2H, Ar, *J* = 7 Hz and *J* = 1.5 Hz), 7.47 (dt, 2H, Ar, *J* = 8 Hz and *J* = 1.5 Hz), 8.11 (s, 2H, -CH=); <sup>13</sup>C NMR (DMSO-*d*<sub>6</sub>, 125 MHz)  $\delta$ : 48.04 (-CH<sub>2</sub>-), 55.77 (-OCH<sub>3</sub>), 111.98 (Ar), 120.75 (TZD), 121.03 (Ar), 121.12 (Ar), 128.84 (-CH=), 129.08 (Ar), 132.92 (Ar), 158.03 (Ar), 166.98 (TZD C=O), 165.79 (TZD C=O), 195.79 (C=O).

(*Z*)-3,3'-(2-oxopropane-1,3-diyl)bis(5-((*Z*)-4-methoxybenzylidene)thiazolidine-2,4-dione) (**5e**): off yellow solid; mp = 276 - 277°C; yield = 70%; IR (KBr)  $\nu_{\max}$  cm<sup>-1</sup>: 1734 (C=O), 1689 (C=O), 1671 (C=O), 1591 (C=C), 1264 (Ar-O-C), 1027 (Ar-O-C); MS: *m/z* = 525.7 (M+1); <sup>1</sup>H NMR (DMSO-*d*<sub>6</sub>, 500 MHz)  $\delta$ : 3.83 (s, 6H, -OCH<sub>3</sub>), 4.99 (s, 4H, -CH<sub>2</sub>-), 7.13 (d, 4H, Ar, *J* = 7.5 Hz), 7.61 (d, 4H, Ar, *J* = 7.5 Hz), 7.95 (s, 2H, -CH=); <sup>13</sup>C NMR (DMSO-*d*<sub>6</sub>, 125 MHz)  $\delta$ : 48.22 (-CH<sub>2</sub>-), 56.03 (-OCH<sub>3</sub>), 115.20 (Ar), 125.81 (TZD), 129.41 (-CH=), 131.18 (Ar), 132.54 (Ar), 160.18 (Ar), 165.09 (TZD C=O), 166.16 (TZD C=O), 195.19 (C=O).

(*Z*)-3,3'-(2-oxopropane-1,3-diyl)bis(5-((*Z*)-4-chlorobenzylidene)thiazolidine-2,4-dione) (**5f**): white solid; mp = 290°C dec; yield = 80%; IR (KBr)  $\nu_{\max}$  cm<sup>-1</sup>: 1739 (C=O), 1700 (C=O), 1681 (C=O), 1609 (C=C), 520 (C-Cl); MS: *m/z* = 533.0 (M+1); <sup>1</sup>H NMR (DMSO-*d*<sub>6</sub>, 500 MHz)  $\delta$ : 4.97 (s, 4H, -CH<sub>2</sub>-), 7.65 - 7.66 (m, 8H, Ar), 7.99 (s, 2H, -CH=); <sup>13</sup>C NMR (DMSO-*d*<sub>6</sub>, 125 MHz)  $\delta$ : 48.19 (-CH<sub>2</sub>-), 123.16 (-CH=), 123.90 (TZD), 129.48 (Ar), 131.71 (Ar), 132.09 (Ar), 136.14 (Ar), 164.31 (TZD C=O), 166.56 (TZD C=O), 195.70 (C=O).

(*Z*)-3,3'-(2-oxopropane-1,3-diyl)bis(5-((*Z*)-3-chlorobenzylidene)thiazolidine-2,4-dione) (**5g**): white solid; mp = 282°C dec; yield = 56%; IR (KBr)  $\nu_{\max}$  cm<sup>-1</sup>: 1736 (C=O), 1699 (C=O), 1686 (C=O), 1606 (C=C), 677 (C-Cl); MS: *m/z* = 550.1 (M+1); <sup>1</sup>H NMR (DMSO-*d*<sub>6</sub>, 500 MHz)  $\delta$ : 5.01 (s, 4H, -CH<sub>2</sub>-), 7.57 - 7.61 (m, 6H, Ar), 7.75 (s, 2H, Ar), 7.99 (s, 2H, -CH=); <sup>13</sup>C NMR (DMSO-*d*<sub>6</sub>, 125 MHz)  $\delta$ : 48.18 (-CH<sub>2</sub>-), 122.48 (TZD), 127.83 (-CH=), 130.15 (Ar), 130.40 (Ar), 131.20 (Ar), 132.27 (Ar), 133.97 (Ar), 134.91 (Ar), 164.67 (TZD C=O), 166.37 (TZD C=O), 195.65 (C=O).

(*Z*)-3,3'-(2-oxopropane-1,3-diyl)bis(5-((*Z*)-2,4-dichlorobenzylidene)thiazolidine-2,4-dione) (**5h**): white solid; mp = 300 - 301°C; yield = 76%; IR

(KBr)  $\nu_{\max}$  cm<sup>-1</sup>: 1742 (C=O), 1706 (C=O), 1701 (C=O), 1602 (C=C), 722 (C-Cl), 502 (C-Cl); MS: *m/z* = 601.9 (M+1); <sup>1</sup>H NMR (DMSO-*d*<sub>6</sub>, 500 MHz)  $\delta$ : 4.99 (s, 4H, -CH<sub>2</sub>-), 7.50 (s, 2H, Ar), 7.67 - 7.70 (m, 4H, Ar), 7.85 (s, 2H, -CH=); <sup>13</sup>C NMR (DMSO-*d*<sub>6</sub>, 125 MHz)  $\delta$ : 48.79 (-CH<sub>2</sub>-), 125.15 (-CH=), 126.20 (TZD), 128.98 (Ar), 130.94 (Ar), 131.20 (Ar), 131.66 (Ar), 135.99 (Ar), 136.03 (Ar), 165.08 (TZD C=O), 167.11 (TZD C=O), 195.39 (C=O).

(5*Z*,5'*Z*)-3,3'-(2-oxopropane-1,3-diyl)bis(5-(pyridin-3-ylmethylene)thiazolidine-2,4-dione) (**5i**): orange-brick solid; mp = 279°C dec; yield = 94%; IR(KBr)  $\nu_{\max}$  cm<sup>-1</sup>: 1733 (C=O), 1705 (C=O), 1689 (C=O), 1621 (C=C); MS: *m/z* = 467.2 (M+1); <sup>1</sup>H NMR (DMSO-*d*<sub>6</sub>, 500 MHz)  $\delta$ : 5.02 (s, 4H, -CH<sub>2</sub>-), 7.59 (dd, 2H, Py, *J* = 5 Hz and *J* = 4.5 Hz), 8.01 (m, 2H, Py), 8.03 (s, 2H, -CH=), 8.66 (d, 2H, Py, *J* = 4.5 Hz), 8.89 (s, 2H, Py); <sup>13</sup>C NMR (DMSO-*d*<sub>6</sub>, 125 MHz)  $\delta$ : 48.21 (-CH<sub>2</sub>-), 122.89 (TZD), 124.22 (-CH=), 128.91 (Py), 130.64 (Py), 136.17 (Py), 150.88 (Py), 151.44 (Py), 164.61 (TZD C=O), 166.31 (TZD C=O), 195.62 (C=O).

(5*Z*,5'*Z*)-3,3'-(2-oxopropane-1,3-diyl)bis(5-(thiophen-3-ylmethylene)thiazolidine-2,4-dione) (**5j**): off white solid; mp = 280°C dec; yield = 90%; IR (KBr)  $\nu_{\max}$  cm<sup>-1</sup>: 1736 (C=O), 1695 (C=O), 1680 (C=O), 1597 (C=C); MS: *m/z* = 477.0 (M+1); <sup>1</sup>H NMR (DMSO-*d*<sub>6</sub>, 500 MHz)  $\delta$ : 5.01 (s, 4H, -CH<sub>2</sub>-), 7.20 (m, 2H, Tf), 7.59 (d, 2H, Tf), 7.89 (d, 2H, Tf), 8.11 (s, 2H, -CH=); <sup>13</sup>C NMR (DMSO-*d*<sub>6</sub>, 125 MHz)  $\delta$ : 48.73 (-CH<sub>2</sub>-), 122.31 (TZD), 123.21 (-CH=), 125.45 (Tf), 126.19 (Tf), 132.61 (Tf), 133.07 (Tf), 164.74 (TZD C=O), 166.33 (TZD C=O), 195.32 (C=O).

#### Molecular docking

To evaluate the potential affinity of the compounds **5a-j** to K-Ras, N-Ras and B-Raf, a molecular docking study was performed. The results were expressed as the variation of Gibbs free energy ( $\Delta G$ ) for each ligand-macromolecule interaction obtained from both AutoDock vina 1.1.2 and AutoDock 4.2. The numeric results are presented in Table I.

The higher affinity of the compounds **5a-j** was found to be to K-Ras and in a slightly lower way, to B-Raf. The affinity for N-Ras was found to be low on both software used, indicating that targeting of this protein with this class of compounds is unlikely to happen and no more analysis or research on targeting N-Ras was performed in this paper. The best correlation between the binding affinities given by AutoDock vina and AutoDock follow was found for K-Ras ( $R^2 = 0.86$ ), providing the highest cross-validation of data from the present results and were further subjected to a molecular dynamics study to confirm the hypothesis of binding of the top (Q1) compounds (**5b** and **5h**) to K-Ras.

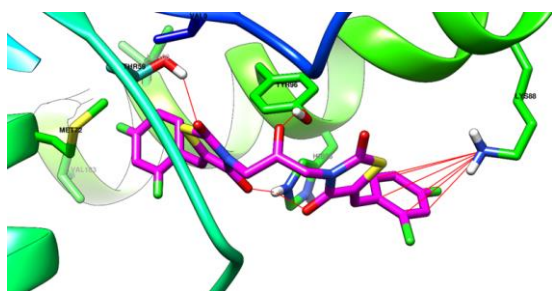
**Table I**

The binding affinity of the studied compounds to K-Ras, N-Ras and B-Raf, expressed as variation of the Gibbs free energy (kcal/mol)

Compound	K-Ras		N-Ras		B-Raf	
	ADV	AD	ADV	AD	ADV	AD
<b>5a</b>	-10.0	-10.1	-6.9	-7.0	-9.8	-10.4
<b>5b</b>	<b>-10.3</b>	-10.4	-6.9	-6.9	-9.8	-9.9
<b>5c</b>	-9.7	-9.8	-5.9	-6.2	-9.6	-10.0
<b>5d</b>	-10.0	-10.0	-6.6	-6.7	<b>-9.9</b>	-11.1
<b>5e</b>	-9.4	-9.5	-5.0	-6.8	-8.8	-10.0
<b>5f</b>	-10.1	-10.7	-6.1	-7.2	-9.7	-10.4
<b>5g</b>	-10.2	-10.6	-6.9	-6.9	<b>-10.0</b>	-11.0
<b>5h</b>	<b>-10.8</b>	-11.6	-6.8	-7.6	<b>-10.2</b>	-12.2
<b>5i</b>	-9.8	-9.9	-6.9	-6.8	-9.7	-10.6
<b>5j</b>	-9.1	-9.5	-5.8	-6.4	-9.1	-9.9
<b>R<sup>2</sup></b>	<b>0.86</b>		0.16		0.50	

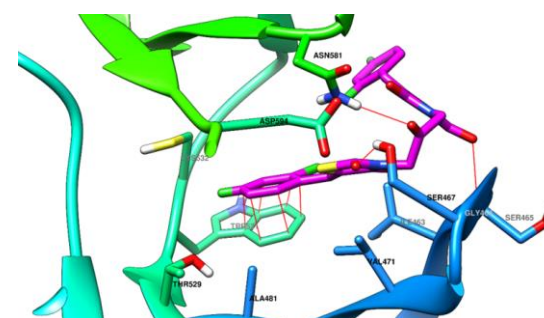
The binding affinities computed by ADV for the compounds that are found in the top Q1, were highlighted in the table

The highest affinity was identified for K-Ras and B-Raf, for the compound **5h**. Its molecular interactions with the two proteins are depicted in Figure 2 and Figure 3. The affinity of compounds **5a-j** to K-Ras is overall the highest from the three studied targets. It can be seen that the preferred substitution of the benzylidene ring is with halogenated atoms (**5b**, **5f-h**) and not with methoxy or nitro (**5c**, **5f**, **5e**) groups. Another improper way is the replacement of the benzylidene ring with a pyridine (**5i**) or thiophene (**5j**).

**Figure 2.**

The top binding conformation of compound **5h** in the pocket of K-Ras, predicted by AutoDock vina 1.1.2

The best binding compound (**5h**) was predicted to have many interactions with the protein. One of the benzene rings interacts with the positive charged side chain of Lys88, in a  $\pi$ -cation interaction type. The other benzene ring fits in a hydrophobic pocket comprised of Val9, Ile100, Met72 and Val103. The ketone of the ligand is expected to act as an acceptor in a hydrogen bond, with the sidechain of Tyr96. The slightly protonated His96 is expected to interact with the imide oxygen from the position 4 of thiazolidinedione, while the other oxygen acts as acceptor of a hydrogen bond from Thr58. The interaction pattern provided for **5h** with K-Ras is similar for the other compounds from the present series (data not provided). Analysis of the binding energies of the compounds in the binding site of B-Raf leads to some observations

**Figure 3.**

The top binding conformation of compound **5h** in the pocket of B-Raf, predicted by AutoDock vina 1.1.2

In the studied pocket of the protein, two types of regions were identified – one polar region and one hydrophobic region. The outer region is the polar one, comprised of some polar residues: Asp594, Asn581, Ser467 and Ser465, where the polyketonic zone of the studied compounds would interact with.

One of the benzylidene rings of the molecule would interact with Trp531 by  $\pi$ - $\pi$  stacking, while with other amino acid residues (Ala481, Val471, Ile463), there would be hydrophobic interactions.

Analysis of the binding poses indicated that substitution in position *para* of the aromatic ring (especially if the substituent is bulky), could interfere in a negative way with the loop Gln530-Cys532, pushing the thiazolidinedione out of the polar region, making the polar interactions less favourable.

*Molecular dynamics simulation*

The most promising interaction pattern between the present series of compounds and the studied proteins lead to the possibility that the compounds would bind to K-Ras. Therefore, for the compounds which exhibited the highest affinity to K-Ras (**5b** and **5h**), a molecular dynamics study was performed in order to evaluate the stability of the predicted complexes of those compounds with K-Ras. As stated above, the best binding pose predicted by AutoDock vina 1.1.2 was taken and studied in the current molecular dynamics study. After the simulation of 100 ns of the complexes and the apo form of the protein, the results of the trajectories were analysed.

In Figure 4, there is depicted the root mean square deviation (RMSD) of K-Ras in its apo form, compared when it is complexed with **5b** and **5h**. It can be seen that the apo protein reaches a plateau after 60 ns, while the two complexed ones have a different behaviour. After about 30 ns, the complex with **5b** reaches a plateau, while the complex with **5h** does not reach the convergence; the RMSD fluctuates, with a slight tendency to increase. This observation should be connected with the number of hydrogen bonds between the two ligands and K-Ras. While between compound **5b** and K-Ras it can be found an average of 2 hydrogen bonds during the simulation, compound **5h** would leave the binding pocket after approximately 20 ns (Figure 5).

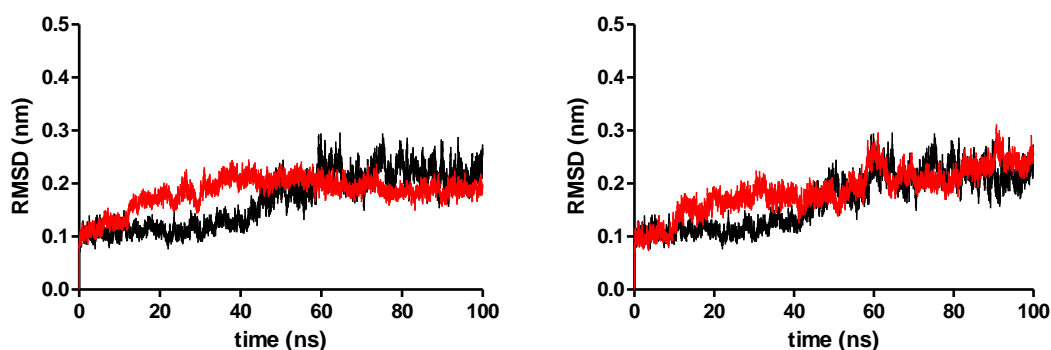


**Figure 4.**

The RMSD of K-Ras after the molecular dynamics simulation. In black is the apo form, while in red are represented the complexes with **5b** (left) and **5h** (right)

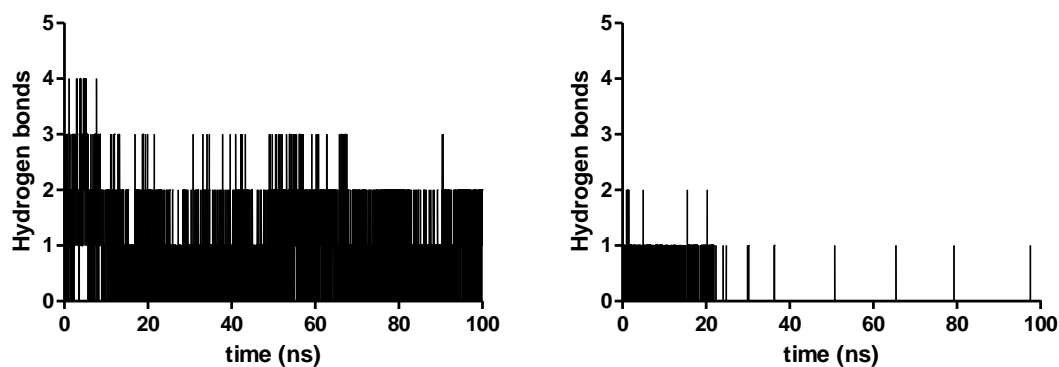


**Figure 5.**

The number of hydrogen bonds between K-Ras and **5b** (left) and **5h** (right) after the molecular dynamics simulation

## Conclusions

We synthesized a series of new hybrid molecules, with a symmetrical chemical structure, in which two identical 5-arylidene-thiazolidine-2,4-dione moieties are linked through a propanone fragment. The methods used for their structural characterization confirmed the obtaining of di-thiazolidinediones and not of the mono-thiazolidinediones. The *in silico* study showed the affinity of the new molecules to bind more to K-Ras oncoprotein. The results of the molecular dynamics simulation done on compounds **5b** and **5h**, which had the highest affinity for K-Ras, state that this approach

is necessary to confirm the results of the molecular docking studies, because some of the ligands with good binding properties, would not make stable complexes, in time. The complementarity between the two *in silico* techniques would remove the well-known false positives from the results of the molecular docking study. This research will be completed with testing of the obtained compounds on cancer cell lines with K-Ras mutation, with the aim of determining the levels of correlation of the *in silico* data with the *in vitro* results.

## Acknowledgement

This research was funded by “Iuliu Hațieganu” University of Medicine and Pharmacy, Cluj-Napoca, Romania, grant number 35182/17.12.2021 and by the MCID through the “Nucleu” Program within the National Plan for Research, Development and Innovation 2022-2027, project PN 23 24 01 05.

## Conflict of interest

The authors declare no conflict of interest.

## References

- Asati V, Mahapatra DK, Bharti SK, Thiazolidine-2,4-diones as multi-targeted scaffold in medicinal chemistry: Potential anticancer agents. *Eur J Med Chem.*, 2014; 87: 814-833.
- Bauer P, Hess B, Lindahl L, GROMACS 2022 Source code (Version 2022). Zenodo, 2022.
- Berman HM, Westbrook J, Feng Z, Gilliland G, Bhat TN, Weissig H, Shindyalov IN, Bourne PE, The Protein Data Bank. *Nucleic Acids Res.*, 2000; 28(1): 235-242.
- Bhanushali U, Rajendran S, Sarma K, Kulkarni P, Chatti K, Chatterjee S, Ramaa CS, 5-Benzylidene-2,4-thiazolidinedione derivatives: Design, synthesis and evaluation as inhibitors of angiogenesis targeting VEGFR-2. *Bioorg Chem.*, 2016; 67: 139-147.
- Blanquicett C, Roman J, Hart CM, Thiazolidinediones as anti-cancer agents. *Cancer Ther.*, 2008; 6(A): 25-34.
- Bray F, Laversanne M, Weiderpass E, Soerjomataram I, The ever-increasing importance of cancer as a leading cause of premature death worldwide. *Cancer*, 2021; 127(16): 3029-3030.
- Cellai I, Petrangolini G, Tortoreto M, Pratesi G, Luciani P, Deledda C, Benvenuti S, Ricordati C, Gelmini S, Ceni E, Galli A, Balzi M, Faraoni P, Serio M, Peri A, *In vivo* effects of rosiglitazone in a human neuroblastoma xenograft. *Br J Cancer*, 2010; 102(4): 685-692.
- Chang S, Lee J, Oh H, Kim U, Ryu B, Park J, Troglitazone inhibits the migration and invasion of PC-3 human prostate cancer cells by upregulating E-cadherin and glutathione peroxidase 3. *Oncol Lett.*, 2018; 16(4): 5482-5488.
- Claudio Viegas-Junior, Eliezer J. Barreiro, Carlos Alberto Manssour Fraga, Molecular Hybridization: A Useful Tool in the Design of New Drug Prototypes. *Curr Med Chem.*, 2007; 14(17): 1829-1852.
- Elrod HA, Sun SY, PPAR  $\gamma$  and Apoptosis in Cancer. *PPAR Res.*, 2008; 2008: 1-12.
- Elstner E, Müller C, Koshizuka K, Williamson EA, Park D, Asou H, Shintaku P, Said JW, Heber D, Koeffler HP, Ligands for peroxisome proliferator-activated receptor  $\gamma$  and retinoic acid receptor inhibit growth and induce apoptosis of human breast cancer cells *in vitro* and in BNX mice. *Proc Natl Acad Sci.*, 1998; 95(15): 8806-8811.
- Ferruzzi P, Ceni E, Tarocchi M, Grappone C, Milani S, Galli A, Fiorelli G, Serio M, Mannelli M, Thiazolidinediones Inhibit Growth and Invasiveness of the Human Adrenocortical Cancer Cell Line H295R. *J Clin Endocrinol Metab.*, 2005; 90(3): 1332-1339.
- Fershtat LL, Makhova NN, Molecular Hybridization Tools in the Development of Furoxan-Based NO-Donor Prodrugs. *ChemMedChem.*, 2017; 12(9): 622-638.
- Grommes C, Landreth GE, Heneka MT, Antineoplastic effects of peroxisome proliferator-activated receptor  $\gamma$  agonists. *Lancet Oncol.*, 2004; 5(7): 419-429.
- Hanwell MD, Curtis DE, Lonie DC, Vandermeersch T, Zurek E, Hutchison GR, Avogadro: an advanced semantic chemical editor, visualization, and analysis platform. *J Cheminform.*, 2012; 4(1): 17.
- Higuchi T, Sugisawa N, Miyake K, Oshiro H, Yamamoto N, Hayashi K, Kimura H, Miwa S, Igarashi K, Kline Z, Bouvet M, Singh SR, Tsuchiya H, Hoffman RM, Pioglitazone, an agonist of PPAR $\gamma$ , reverses doxorubicin-resistance in an osteosarcoma patient-derived orthotopic xenograft model by downregulating P-glycoprotein expression. *Biomed Pharmacother.*, 2019; 118: 109356.
- Huang J, MacKerell AD, CHARMM36 all-atom additive protein force field: Validation based on comparison to NMR data. *J Comput Chem.*, 2013; 34(25): 2135-2145.
- Irina C. Chiș, Clichici A, Simearea R, Moldovan R, Leordean Lazar V, Clichici S, Oniga O, Nastasă C, The effects of a new chromenyl-methylenethiazolidine-2,4-dione in alleviating oxidative stress in a rat model of streptozotocin induced diabetes. *Stud Univ Babeș-Bolyai Chem.*, 2018; 63(4):103-112.
- Jin H, Zhou Z, Wang D, Guan S, Han W, Molecular Dynamics Simulations of Acylpeptide Hydrolase Bound to Chlorpyrifosmethyl Oxon and Dichlorvos. *Int J Mol Sci.*, 2015; 16(12): 6217-6234.
- Jin JQ, Han JS, Ha J, Baek HS, Lim DJ, Lobeglitazone, A Peroxisome Proliferator-Activated Receptor-Gamma Agonist, Inhibits Papillary Thyroid Cancer Cell Migration and Invasion by Suppressing p38 MAPK Signaling Pathway. *Endocrinol Metab.*, 2021; 36(5): 1095-1110.
- Jorgensen WL, Chandrasekhar J, Madura JD, Impey RW, Klein ML, Comparison of simple potential functions for simulating liquid water. *J Chem Phys.*, 1983; 79(2): 926-935.
- Karoulia Z, Wu Y, Ahmed TA, Xin Q, Bollard J, Krepler C, Wu X, Zhang C, Bollag G, Herlyn M, Fagin JA, Lujambio A, Gavathiotis E, Poulikakos PI, An Integrated Model of RAF Inhibitor Action Predicts Inhibitor Activity against Oncogenic BRAF Signaling. *Cancer Cell.*, 2016; 30(3): 485-498.
- Kessler D, Bergner A, Böttcher J, Fischer G, Döbel S, Hinkel M, Müllauer B, Weiss-Puxbaum A, McConnell DB, Drugging all RAS isoforms with one pocket. *Future Med Chem.*, 2020; 12(21): 1911-1923.
- Khanjiwala Z, Khale A, Prabhu A, Docking structurally similar analogues: Dealing with the false-positive. *J Mol Graph Model*, 2019; 93: 107451.
- Liu K, Rao W, Parikh H, Li Q, Guo TL, Grant S, Kellogg GE, Zhang S, 3,5-Disubstituted-thiazolidine-2,4-dione analogs as anticancer agents: design, synthesis and biological characterization. *Eur J Med Chem.*, 2012; 47(1): 125-137.



26. Lu H, The effect of pioglitazone on intimal hyperplasia of venous bridge vascular. *Farmacia*, 2020; 68(5): 905-911.
27. Lv Z, Wang HS, Niu XD, Molecular dynamics simulations reveal insight into key structural elements of aaptamines as sortase inhibitors with free energy calculations. *Chem Phys Lett.*, 2013; 585: 171-177.
28. Makeneni S, Thieker DF, Woods RJ, Applying Pose Clustering and MD Simulations To Eliminate False Positives in Molecular Docking. *J Chem Inf Model*, 2018; 58(3): 605-614.
29. Mao Z, Xiao H, Shen P, Yang Y, Xue J, Yang Y, Shang Y, Zhang L, Li X, Zhang Y, Du Y, Chen CC, Guo RT, Zhang Y, KRAS(G12D) can be targeted by potent inhibitors *via* formation of salt bridge. *Cell Discov.*, 2022; 8(1): 5.
30. Marc G, Oniga SD, Pirnău A, Duma M, Vlase L, Oniga O, Rational Synthesis of Some New para-Aminobenzoic Acid Hybrids with Thiazolidin-2,4-diones with Antimicrobial Properties ADMET and molecular docking evaluation. *Rev Chim.*, 2019; 70(3): 769-775.
31. Marc G, Stana A, Oniga SD, Pirnău A, Vlase L, Oniga O, New Phenolic Derivatives of Thiazolidine-2,4-dione with Antioxidant and Antiradical Properties: Synthesis, Characterization, *In Vitro* Evaluation, and Quantum Studies. *Molecules*, 2019; 24(11): 2060.
32. Marc G, Stana A, Pirnău A, Vlase L, Oniga S, Oniga O, Regioselectivity evaluation of the (Z)-5-(4-hydroxybenzylidene)-thiazolidine-2,4-dione alkylation in alkaline environment. *J Mol Struct.*, 2021; 1241: 130629.
33. McCubrey JA, Steelman LS, Chappell WH, Abrams SL, Franklin RA, Montalto G, Cervello M, Libra M, Candido S, Malaponte G, Mazzarino MC, Fagone P, Nicoletti F, Bäsecke J, Mijatovic S, Maksimovic-Ivanic D, Milella M, Tafuri A, Chiarini F, Evangelisti C, Cocco L, Martelli AM, Ras/Raf/MEK/ERK and PI3K/PTEN/Akt/mTOR Cascade Inhibitors: How Mutations Can Result in Therapy Resistance and How to Overcome Resistance. *Oncotarget*, 2012; 3(10): 1068-1111.
34. Monami M, Dicembrini I, Mannucci E, Thiazolidinediones and cancer: results of a meta-analysis of randomized clinical trials. *Acta Diabetol.*, 2014; 51(1): 91-101.
35. Morris GM, Huey R, Lindstrom W, Sanner MF, Belew RK, Goodsell DS, Olson AJ, AutoDock4 and AutoDockTools4: Automated Docking with Selective Receptor Flexibility. *J Comput Chem.*, 2009; 30(16): 2785-2791.
36. Nastasă C, Duma M, Tipericiu B, Oniga O, Antimicrobial screening of new 5-(chromene-3-yl)methylene-2,4-thiazolidinediones. *Bangladesh J Pharmacol.*, 2015; 10(3): 716.
37. Nastasă C, Tamaian R, Oniga O, Tipericiu B, 5-Arylidene(chromenyl-methylene)-thiazolidinediones: Potential New Agents against Mutant Oncoproteins K-Ras, N-Ras and B-Raf in Colorectal Cancer and Melanoma. *Medicina (B Aires)*, 2019; 55(4): 85.
38. Nastasă C, Tipericiu B, Pârnu A, Duma M, Ionuț I, Oniga O, Synthesis of New N-Substituted 5-Arylidene-2,4-thiazolidinediones as Anti-Inflammatory and Antimicrobial Agents. *Arch Pharm (Weinheim)*, 2013; 346(6): 481-490.
39. Ninomiya I, Yamazaki K, Oyama K, Hayashi H, Tajima H, Kitagawa H, Fushida S, Fujimura T, Ohta T, Pioglitazone inhibits the proliferation and metastasis of human pancreatic cancer cells. *Oncol Lett.*, 2014; 8(6): 2709-2714.
40. Nirwan S, Chahal V, Kakkar R, Thiazolidinones: Synthesis, Reactivity, and Their Biological Applications. *J Heterocycl Chem.*, 2019; 56(4): 1239-1253.
41. O'Boyle NM, Banck M, James CA, Morley C, Vandermeersch T, Hutchison GR, Open Babel: An open chemical toolbox. *J Cheminform.*, 2011; 3(1): 33.
42. Pop B, Ionuț I, Marc G, Vodnar DC, Pirnău A, Vlase L, Oniga O, Development of new 2-methyl-4-salicylamide thiazole derivatives: synthesis, antimicrobial activity evaluation, lipophilicity and molecular docking study. *Farmacia*, 2021; 69(4):724-731.
43. Reka AK, Kurapati H, Narala VR, Bommer G, Chen J, Standiford TJ, Keshamouni VG, Peroxisome Proliferator-Activated Receptor- $\gamma$  Activation Inhibits Tumor Metastasis by Antagonizing Smad3-Mediated Epithelial-Mesenchymal Transition. *Mol Cancer Ther.*, 2010; 9(12): 3221-3232.
44. Rousselot P, Prost S, Guilhot J, Roy L, Etienne G, Legros L, Charbonnier A, Coiteux V, Cony-Makhoul P, Huguet F, Cayssials E, Cayuela J, Relouzat F, Delord M, Bruzzoni-Giovanelli H, Morisset L, Mahon F, Guilhot F, Leboulch P, Pioglitazone together with imatinib in chronic myeloid leukemia: A proof of concept study. *Cancer*, 2017; 123(10): 1791-1799.
45. Seabloom DE, Galbraith AR, Haynes AM, Antonides JD, Wuertz BR, Miller WA, Miller KA, Steele VE, Miller MS, Clapper ML, O'Sullivan MG, Ondrey FG, Fixed-Dose Combinations of Pioglitazone and Metformin for Lung Cancer Prevention. *Cancer Prev Res.*, 2017; 10(2): 116-123.
46. Shelke KF, Sapkal SB, Kakade GK, Sadaphal SA, Shingate BB, Shingare MS, Alum catalyzed simple and efficient synthesis of 5-arylidene-2,4-thiazolidinedione in aqueous media. *Green Chem Lett Rev.*, 2010; 3(1): 17-21.
47. Smallridge RC, Copland JA, Brose MS, Wadsworth JT, Houvras Y, Menefee ME, Bible KC, Shah MH, Gramza AW, Klopffer JP, Marlow LA, Heckman MG, Von Roemeling R, Efatutazone, an Oral PPAR- $\gamma$  Agonist, in Combination With Paclitaxel in Anaplastic Thyroid Cancer: Results of a Multicenter Phase 1 Trial. *J Clin Endocrinol Metab.*, 2013; 98(6): 2392-2400.
48. Tilekar K, Upadhyay N, Hess JD, Macias LH, Mrowka P, Aguilera RJ, Meyer-Almes FJ, Iancu CV, Choe J, Ramaa CS, Structure guided design and synthesis of furyl thiazolidinedione derivatives as inhibitors of GLUT 1 and GLUT 4, and evaluation of their anti-leukemic potential. *Eur J Med Chem.*, 2020; 202: 112603.
49. Trott O, Olson AJ, AutoDock Vina: Improving the speed and accuracy of docking with a new scoring function, efficient optimization, and multithreading. *J Comput Chem.*, 2009; 31(2): 455-461.
50. Turkevich NM, Steblyuk PN, Vladzimirskaya EV, Zdorenko VA, Synthesis and antimicrobial activity of compounds with two thiazolidine rings. *Pharm Chem J.*, 1978; 12(11): 1456-1459.

51. Upadhyay N, Tilekar K, Jänsch N, Schweipert M, Hess JD, Henze Macias L, Mrowka P, Aguilera RJ, Choe J, Meyer-Almes FJ, Ramaa CS, Discovery of novel N-substituted thiazolidinediones (TZDs) as HDAC8 inhibitors: *in-silico* studies, synthesis, and biological evaluation. *Bioorg Chem.*, 2020; 100: 103934.
52. Upadhyay N, Tilekar K, Loiodice F, Anisimova NY, Spirina TS, Sokolova D V, Smirnova GB, Choe J, Meyer-Almes FJ, Pokrovsky VS, Lavecchia A, Ramaa C, Pharmacophore hybridization approach to discover novel pyrazoline-based hydantoin analogs with anti-tumor efficacy. *Bioorg Chem.*, 2021; 107: 104527.
53. Wang X, Zhang H, Chen X, Drug resistance and combating drug resistance in cancer. *Cancer Drug Resist.*, 2019; 2(2): 141-160.
54. Wei S, Yang J, Lee SL, Kulp SK, Chen CS, PPAR $\gamma$ -independent antitumor effects of thiazolidinediones. *Cancer Lett.*, 2009; 276(2): 119-124.
55. Yang DH, Chen ZC, Chen SY, Zheng QG, A convenient synthesis of 5-benzylidenethiazolidine-2,4-diones under microwave irradiation without solvent. *J Chem Res.*, 2003; (S): 330-331.